Project: **Anti-CASPR1 antibody pathogenicity and immune functions of the node of *Ranvier***

Principal investigators: Luis Querol, MD, PhD; Laura Batlle, PhD
Postdoctoral researchers: Juan Castilla Silgado, PhD; Carmen Menacho Pando, PhD

The first year of the project has been dedicated to establishing the methodological and experimental framework necessary for the successful completion of the proposed objectives. During this period, we have optimized the *in vitro* models required to study anti-CASPR1 pathogenicity, completed key mechanistic assays, established the collaboration with the Centre for Genomic Regulation (CRG) to develop a fully human iPSC-derived myelination model, and prepared the *in vivo* studies through specialized training and submission of the corresponding ethical approval. Overall, the project has achieved the main methodological milestones planned for the first year and is well positioned to initiate the remaining experimental activities during the second year.

Objective 1A: Pathogenicity of anti-CASPR1 antibodies *in vitro* myelinating co-cultures

To investigate the pathogenic effects of anti-CASPR1 antibodies in vitro, we established a primary myelinating neuron–Schwann cell co-culture system using dorsal root ganglia (DRG) isolated from embryonic rats. The culture protocol was optimized to obtain reproducible myelination and proper formation of nodes of Ranvier, including refinement of the dissociation procedure, culture conditions, myelination protocol and immunofluorescence methodology.

The resulting co-cultures consistently generated compact myelin sheaths together with well-organized nodal and paranodal domains, as confirmed by immunostaining for myelin and nodal/paranodal markers (figure 1). Following the successful establishment of this experimental platform, pathogenicity studies using sera and purified IgG from anti-CASPR1-positive patients have been initiated and are currently ongoing. These experiments will evaluate the effects of patient-derived antibodies on paranodal integrity, nodal organization and myelin stability.

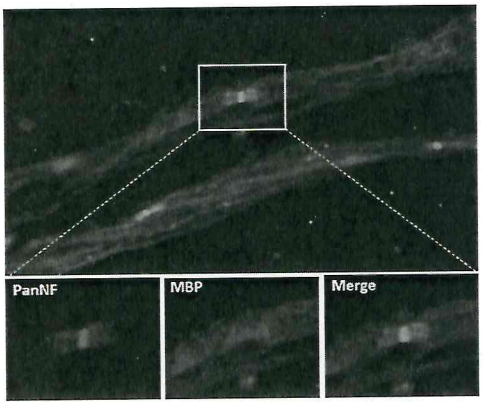


Figure 1. Representative immunofluorescence image of the established primary myelinating DRG neuron–Schwann cell co-culture showing compact myelin (MBP, green) and a well-defined node of Ranvier (pan-neurofascin, red).

Ojective 1B-C. Cell aggregation assays and isotype-dependent pathogenicity of anti-CASPR1 antibodies

To investigate whether anti-CASPR1 antibodies interfere with the interaction between the CASPR1/CNTN1 complex and NF155, we established a HEK293T cell aggregation assay using cells expressing the corresponding axonal and glial proteins. As a first approach, we analyzed the

composition of individual cell aggregates after incubation with purified IgG1 and IgG4 fractions from healthy controls, anti-CNTN1 and anti-CASPR1 patients (Figure 2A).

In healthy controls, the majority of aggregates consisted of mixed populations of NF155- and CASPR1/CNTN1-expressing cells, indicating preserved cell-cell adhesion. As expected, incubation with anti-CNTN1 IgG4 markedly shifted the distribution towards aggregates lacking GFP-positive cells, confirming the previously described disruption of the paranodal interaction and validating the assay. Importantly, both IgG1 and IgG4 fractions from anti-CASPR1 patients also induced a clear redistribution towards aggregates containing fewer GFP-positive cells, demonstrating impaired incorporation of CASPR1/CNTN1-expressing cells into mixed aggregates and supporting a direct effect of anti-CASPR1 antibodies on paranodal cell adhesion.

These observations were confirmed by quantitative analysis of cluster interaction, which demonstrated a significant reduction in mixed cell aggregation following incubation with anti-CASPR1 antibodies compared with healthy controls (Figure 2B). Together, these results provide functional evidence that anti-CASPR1 antibodies impair the interaction between the CASPR1/CNTN1 complex and NF155, further supporting their pathogenic role in autoimmune nodopathies.

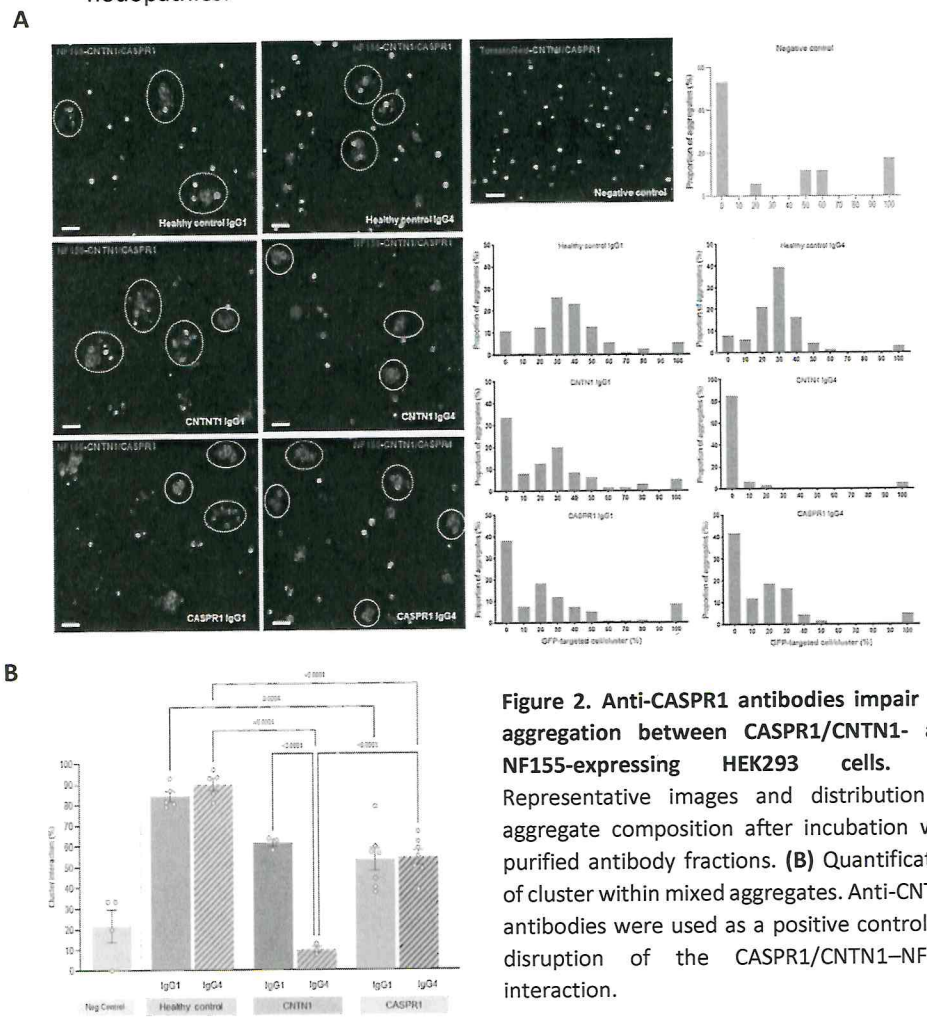


Figure 2. Anti-CASPR1 antibodies impair cell aggregation between CASPR1/CNTN1- and NF155-expressing HEK293 cells. (A) Representative images and distribution of aggregate composition after incubation with purified antibody fractions. **(B)** Quantification of cluster within mixed aggregates. Anti-CNTN1 antibodies were used as a positive control for disruption of the CASPR1/CNTN1–NF155 interaction.

Objective 2: Assessment of immune system molecules in nodes of Ranvier: EAN model

To ensure the successful implementation of the experimental autoimmune neuritis (EAN) model, the postdoctoral researcher Juan Castilla completed a three-month research internship in the laboratory of Dr. Jérôme Devaux (Institute of Functional Genomics, Montpellier, France), an internationally recognized group with extensive expertise in experimental models of autoimmune neuropathies. During this period, specialized training was received in the induction, clinical assessment and histopathological characterization of the EAN model, enabling the transfer and implementation of these methodologies in our laboratory.

In parallel, the complete animal experimentation protocol was designed and submitted for ethical approval. Authorization is currently pending, and the implementation of the EAN model and the subsequent experimental studies will begin immediately upon approval.

Objective 3: Set-up and initial evaluation of a fully human iPSC-derived peripheral myelination system

Substantial progress was made toward establishing a fully human iPSC-derived peripheral myelination system based on motor neurons and Schwann cells. This platform is intended to support future studies of myelin formation, nodal and paranodal organization, and immune-mediated injury.

A project-specific working cryobank of KOLF human iPSCs was first established after adaptation from Matrigel/mTeSR1 to Geltrex/Essential 8 culture conditions. This provides a standardized and reproducible cell source for subsequent differentiation experiments.

For motor neuron generation, an initial differentiation strategy produced a poor neuronal yield and was therefore replaced by a neurosphere-based protocol. This optimized approach generated robust neural progenitor cultures, neurosphere formation, and extensive neurite outgrowth after replating (Figure 3A–B). Immunofluorescence confirmed strong expression of the neuronal markers TUBB3, NF-H, and MAP2 under different coating conditions, supporting successful neuronal differentiation and maturation (Figure 3C). Further characterization using choline acetyltransferase (ChAT) will be performed to confirm motor neuron identity.

In parallel, differentiation toward Schwann cell precursors (SCPs) was initiated using a two-step protocol involving neural induction followed by NRG1-mediated Schwann lineage specification (Figure 4A). Because several methodological details required adaptation to our experimental conditions, different culture and passaging strategies were evaluated. SOX10-positive cells were successfully generated (Figure 4B), and comparison of the different conditions identified a best-performing strategy yielding approximately 8% SOX10-positive cells (Figure 4C), providing an initial benchmark for further optimization.

These experiments identified the generation and expansion of SCPs as the main technical bottleneck. The next phase will therefore focus on optimizing culture conditions, passaging, and expansion procedures to obtain a sufficiently abundant and reproducible progenitor population for terminal Schwann cell differentiation.

Overall, the main milestones achieved during this period include the establishment of a KOLF iPSC cryobank, successful implementation of an improved motor neuron differentiation protocol, generation of neuronal cultures expressing maturation markers, and initial establishment and benchmarking of SCP differentiation. Cryopreserved intermediate stocks have also been generated to support further optimization. The next steps will be to complete motor neuron characterization, improve SCP generation and expansion, and ultimately combine both cell lineages in co-culture to establish a fully human myelinating model suitable for studying node and paranode formation.

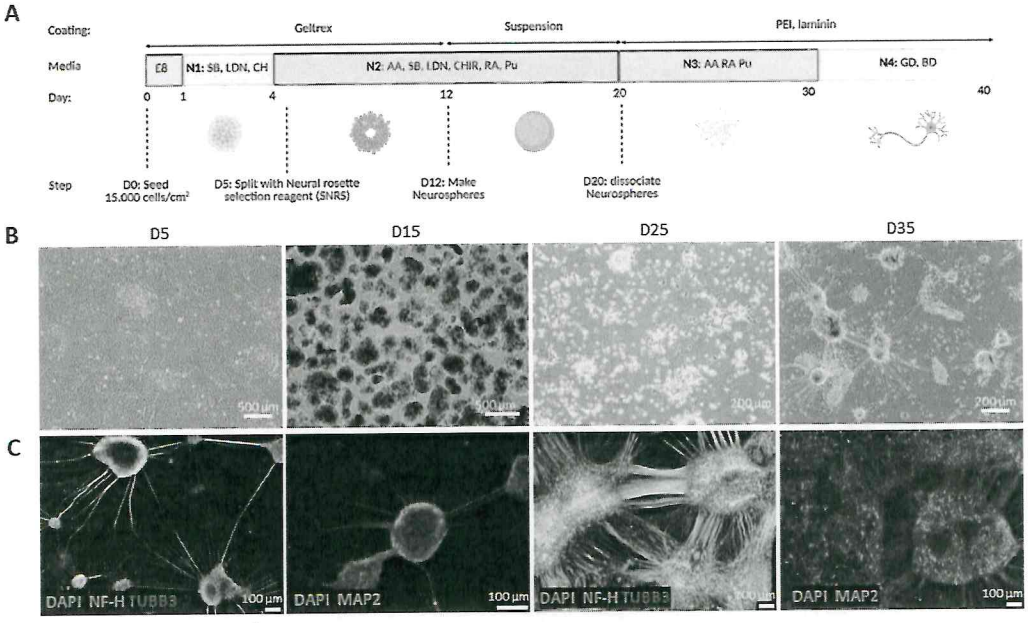


Figure 3. Generation of iPSC-derived motor neurons (MNs) using the new neurosphere-based protocol. (A) Schematic representation of the protocol followed to differentiate hiPSC into motor neurons. **(B)** Four distinctive moments of the protocol: at day 5 for rosette selection, at day 15 after the formation of neurospheres in suspension, at day 25 after dissociation of neurospheres and at day 35 where neurons are grown and connected. **(C)** Representative immunofluorescence shows neuronal networks and neurite outgrowth with NF-H (mature axonal marker), TUBB3 (pan-neuronal marker) and MAP2 (neuronal/dendritic marker) on two different coatings: PEI/laminin (left) and Geltrex (right).

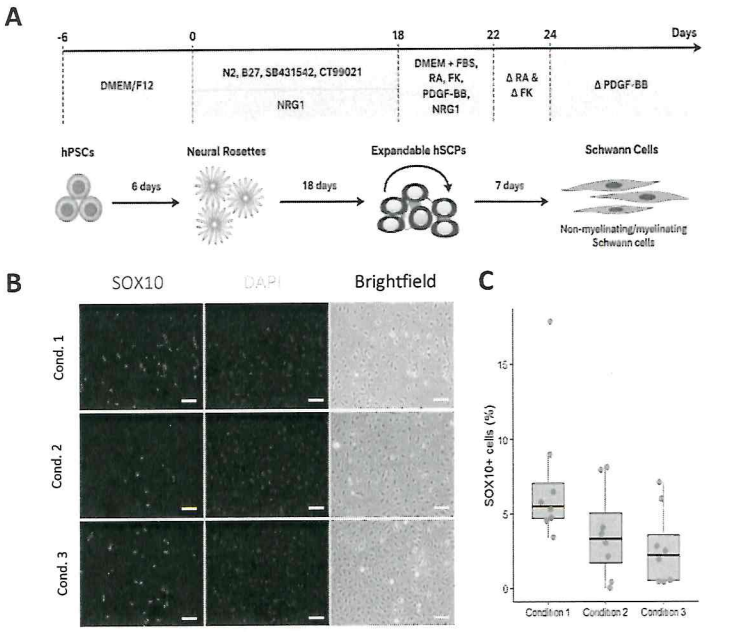


Figure 4. Establishment and optimization of the differentiation protocol for generating iPSC-derived Schwann cell precursors (SCPs). (A) Schematic representation of the differentiation protocol used to generate SCPs from human iPSCs. **(B)** Representative immunofluorescence images of day 18 cultures showing expression of the SCP marker SOX10 (red) and nuclear counterstaining with DAPI (blue), confirming successful induction of the Schwann lineage. Scale bar = 100 µm. **(C)** Quantification of SOX10-positive cells under the different culture conditions tested during protocol optimization. Each dot represents an independent microscopic field from a single differentiation experiment and illustrates the variability between technical replicates used to assess the most suitable differentiation conditions.